A Dynamic Peer-to-Peer Electricity Market Model for a Community Microgrid with Price-Based Demand Response

Fayiz Alfaverh, Mouloud Denai, and Yichuang Sun, *SMIEEE*

Abstract--**Peer-to-Peer (P2P) energy sharing enables prosumers within a community microgrid to directly trade their local energy resources such as solar photovoltaic (PV) panels, small-scale wind turbines, electric vehicle battery storage among each other based on an agreed cost-sharing mechanism. This paper addresses the energy cost minimization problem associated with P2P energy sharing among smart homes which are connected in a residential community. The contribution of this paper is threefold. First, an effective Home Energy Management System (HEMS) is proposed for the smart homes equipped with local generation such as rooftop solar panels, storage and appliances to achieve the demand response (DR) objective. Second, this paper proposes a P2P pricing mechanism based on the dynamic supply-demand ratio and export-import retail prices ratio. This P2P model motivates individual customers to participate in energy trading and ensures that not a single household would be worse off. Finally, the performance of the proposed pricing mechanism, is compared with three popular P2P sharing models in the literature namely the Supply and Demand Ratio (SDR), Mid-Market Rate (MMR) and bill sharing (BS) considering different types of peers equipped with solar panels, electric vehicle, and domestic energy storage system. The proposed P2P framework has been applied to a community consisting of 100 households and the simulation results demonstrate fairness and substantial energy cost saving/revenue among peers. The P2P model has also been assessed under the physical constrains of the distribution network.**

Index Terms— **P2P energy sharing, energy management, vehicle-to-grid, pricing mechanism, demand response.**

I. INTRODUCTION

ELECTRICITY grids across the globe are undergoing a profound transformation from a rigid, fossil-fuel based generation and distribution to a new decentralized low-carbon infrastructure. In this gradual shift towards the adoption of alternative, cleaner and renewable energy sources and smart technology, small-scale consumers have now the control over their energy consumption and are becoming what is known as prosumers (i.e. producers and consumers) [1]. Prosumers can purchase electricity from the grid and sell their energy surplus back to the grid. However, sell back rates or feed-in-tariffs (FiT) remunerations that prosumers receive when selling electricity to the utility are generally much lower than consumer tariffs for the purchase of electricity from the utility [2].

Peer-to-Peer (P2P) energy sharing, where prosumers directly trade their local energy resources with each other without going through an intermediate retailer, has recently emerged as a flexible and cost-effective energy management mechanism which is about to transform the traditional centralized energy market. The P2P electricity model allows prosumers and consumers to initially trade with one another in a local market at a domestic price and then trade with a retailer. The domestic price is generally bounded between the retail price and the export price. As a result, peers can generate revenue from P2P energy exchange regardless of whether they are sellers or buyers of electricity.

The main advantage of the P2P energy exchange is that the locally generated electricity from renewable sources will not to be transported which will ultimately reduce transmission losses and the overall operation costs of the power system. Besides the monetary benefits it offers to consumers and prosumers, P2P electricity trading contributes substantially to increasing the deployment of renewable energy sources. Moreover, the adoption of P2P makes the community more resilient to power outages and improves electricity access to members of the community.

Creating a localized P2P energy market may also be beneficial to the power grid. P2P trading platforms enable an optimal management of decentralized generations through balancing local electricity demand and supply. Furthermore, an effective P2P energy trading scheme incentivizes end-users to consume electricity from the grid at appropriate times of the day which contributes to peak-load reduction.

A number of P2P energy sharing pilot projects have been developed around the world mainly in Europe such as Piclo in the UK, Vandebron in the Netherland, Sonnen Community in Germany and Yeloha and Mosaic in the US. Some of these projects, such as Peer Energy Cloud and Smart Watts in Germany, worked on the information and communication technologies (ICT) to support the energy sharing. Some other projects, such as TransActive Grid in the US, have developed a P2P platform based on blockchain technology that enables members to trade energy secularly and automatically between each other [3].

Several studies focused on pricing mechanisms for P2P

Corresponding author: Mouloud Denai.
F. Alfaverh, M. Denai and Y. Sun are with the School of Physics, Engineering and Computer Science, University of Hertfordshire, Hatfield, AL10 9AB, UK (e-mail: fa17abh@herts.ac.uk, m.denai@herts.ac.uk, y.sun@herts.ac.uk).

energy sharing. They can be classified in two categories: double auction model [4]-[8] and analytical model [9]-[12]. Using double auction model (DA), the peers (sellers and buyers) can interact between each other to trade their energy in a step-by-step fashion as follows [13]; buyer/seller peers submit their bids/offers to an auctioneer, these bids/offers are then arranged in a decreasing/increasing order. Once bids and offers are ordered, the aggregated supply and demand curves are generated and intersected at an auction price. Therefore, the only peers who can engage in the trading process are buyers/sellers with bids greater than/offers lower than the auction price. While consumers with bids lower than the auction price cannot buy from prosumers with offers higher than the auction price, this means that the total surplus of PV generation after self-consumption will not be completely traded within the community microgrid as discussed in [4][5][6]. To address this issue, continuous double auctions (CDAs) which consists of repeating the DA for a certain number of rounds or within a specified time are proposed in [7][8]. Although CDA has a great scalability and high efficiency for distributed energy transactions, the pricing rule and trading strategies of the CDA have some limitations. Due to different trading prices for a series of P2P trading contracts, the CDA does not ensure fairness among peers, in the sense that buyers/sellers may pay more than/earn less than other peers when buying/selling the same amount of energy [14]. In addition, trading prices decided by the auctioneer exhibit higher variation. Therefore, the CDA model cannot offer a fairer trading price that will stimulate the participation of prosumers in the P2P energy trading, which is the main goal of an ideal trading mechanism [15].

An analytical model refers to pricing the energy generated from Distributed Energy Resources (DERs) in a local market based on certain rules, calculation methods or game theoretic approaches. For example, in [9][10], a supply demand ratio (SDR) is proposed as the ratio of the total renewable energy supply to the total net energy demand in a microgrid, where P2P energy prices are a function of SDR. In [11], the mid-market rate (MMR) mechanism provides the trading price among prosumers at the average of the selling and buying prices set by the retailer, with some adjustment based on the difference between the total energy generation and consumption within the community. The bill sharing (BS) mechanism distributes the total energy costs and income among prosumers within a community based on the amount of each prosumer's energy production and consumption. However, these pricing mechanisms (SDR, MMR and BS) cannot guarantee that every participant in the P2P energy sharing market will generate economic benefits [16]. In addition, none of these pricing mechanisms has considered the impact of dynamic retail electricity prices on the P2P market as more retailers may adopt dynamic prices or implement demand response programs [17]. Therefore, pricing mechanisms must be designed with considering dynamic retailer prices, so that prosumers can participate in demand response programs by scheduling and controlling their household appliances and energy storage via a Home Energy Management System (HEMS).

Despite the large body of literature on P2P sharing, a limited number of studies have focused on the participation of electric vehicles (EVs) [18]. Indeed, EVs could serve as a temporary energy storage and supply power to home appliances via Vehicle-to-home (V2H) technology, and/or feed power to the utility grid using Vehicle-to-Grid (V2G) technology when needed. Therefore, P2P energy market may not only depend on the excess of power from PV generation, but also involves EVs in energy trading during their charging and discharging operations. To enable the participation of EVs in P2P energy markets, an efficient pricing strategy must be adopted to balance the interests of all the players [19].

This paper focuses on energy sharing problem inside a residential community. A P2P pricing mechanism is proposed for a community consisting of 100 households to incentivise individual customers to participate in energy trading and to ensure that not a single household would be worse off with considering the physical network constrains. This will simultaneously generate revenue for the energy sharing coordinator (ESC) to cover the maintenance and service operations costs.

The major contributions of this study are summarised as follows:

- The proposed P2P energy trading market model considers uncertainties in household demands, PV generation and EVs flexibility using Monte-Carlo simulation (MCS).
- A HEMS has been developed to allow households participate in demand response programs and minimise their energy cost, maximise revenue and increase the self-consumption ratio.
- The proposed P2P energy market does not only consider trading the excess of PV generation, but also involves trading the energy stored in EVs batteries during their charging and discharging operations.
- A dynamic P2P energy pricing mechanism is designed based on demand-supply ratio and Real-Time Price (RTP) and Feed-in Tariff (FiT) ratio to ensure fairness between the P2P participants considering of the physical network constraints.

The remaining of the paper is organised as follows: Section 2 presents the model of the residential microgrid components which includes various types of households with their HEMS and the network model in a low-voltage area considering of the physical network constraints. The proposed P2P pricing mechanism is described in Section 3. Section 4 presents the results and discussion. Finally, the conclusions of the paper are summarised in Section 6.

II. MODELLING OF RESIDENTIAL MICROGRID COMPONENTS

A. Household Categories

In this study, a residential network consisting of different types of dwellings equipped with solar photovoltaics (PV) panels, battery energy storage system (BES) and electric vehicle (EV) is considered.

As shown in Fig. 1, electricity flow refers to the flow of electric power between buyers and sellers and cash flow refers to the cost involved, and income generated during the electricity
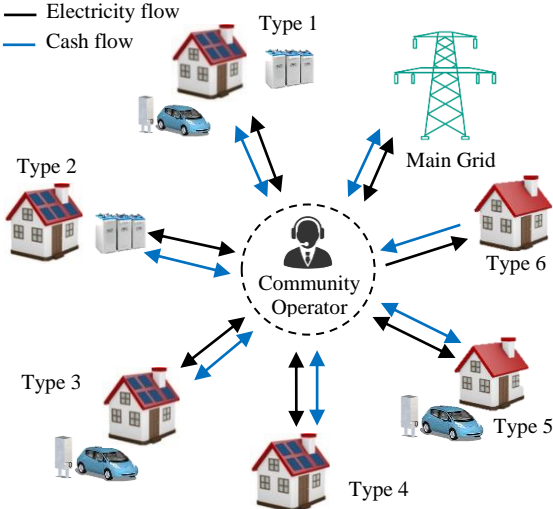
Fig. 1 Different types of households participating in P2P energy sharing.

trade.

The type of household i in the residential microgrid is categorized as $H_j^i, j \in \{1,2,3,4,5,6\}$:

$$H_j^i = \begin{bmatrix} 1 & 1 & 1 \\ 1 & 1 & 0 \\ 1 & 0 & 1 \\ 1 & 0 & 0 \\ 0 & 0 & 1 \\ 0 & 0 & 0 \end{bmatrix} [PV \quad BES \quad EV] \tag{1}$$

Where, matrix entry 1 means household i is equipped with the corresponding device and 0 means the household is not equipped with the corresponding device. Note that households $H_1^i, H_2^i, H_3^i, H_4^i$ and H_5^i could be prosumer (seller or buyer) in the residential microgrid whereas household H_6^i is considered as a consumer (buyer only) all the time.

B. Modelling of household components

1) Modelling of the load and photovoltaic systems: The energy consumption of household i at every time slot over the operation time is defined as:

$$E_L^i(t) \triangleq [E_L^i(1), E_L^i(2), ..., E_L^i(T)] , i \in \{1, 2, ..., N\} \tag{2}$$

Where $\{1, 2, ..., T\}$ is the set of all time slots which are assumed to have equal interval $\Delta t = 5$ min, T denotes the number of time slots over the operation period, and N represents the number of households in the microgrid.

The local PV energy generation of each household during the time interval $[T_s, T_e]$ is defined as:

$$E_{PV}^i(t) \triangleq H_j^i(PV) . [E_{PV}^i(T_s + 1), E_{PV}^i(T_s + 2), ..., E_{PV}^i(T_e)] , 0 < T_s < T_d < T \tag{3}$$

$E_{PV}^i(t)$ represents the PV generation of household i at each time step. $H_j^i(PV)$ indicates whether household i is equipped with PV or not as shown in equation (1) and returns 1 if the household is equipped with PV and 0 otherwise.

2) Modelling of BES: BES enables the excess of power generated from PV to be stored and used later in the day when the solar PV is no longer available. The energy stored in the BES is described by following equation:

$$E_{BES}^i(t) = H_j^i(BES) \Big[E_{BES}^i(t-1)\big(1 - \delta_{SD,BES}^i\big) +$$

$$U_{BES}^i P_{BES,ch}^i(t) \mu_{BES,ch}^i - \frac{(1-U_{BES}^i)P_{BES,dis}^i(t)}{\mu_{BES,dis}^i} \Big] \tag{4}$$

$E_{BES}^i(t)$ and $E_{BES}^i(t-1)$ represent the stored energy at time slot t and $(t-1)$ respectively, δ_{SD}^i is the self-discharging rate, $P_{BES,ch}^i(t)$ and $P_{BES,dis}^i(t)$ denote the battery charging and discharging rates at a given time slot t, respectively, $\mu_{BES,ch}^i$ and $\mu_{BES,dis}^i$ are the charging and discharging efficiencies respectively. $H_j^i(BES)$ indicates whether a BES is available at household i as shown in equation (1) and returns 1 if the household is equipped with BES and 0 otherwise. U_{BES}^i is 1 when the battery is charging and 0 when the battery is discharging. The State of Charge (SoC) of the battery is defined as:

$$\begin{cases} SoC_{BES}^i = \dfrac{E_{BES}^i(t)}{E_{BES,cap}^i} \times 100\% \\ SoC_{BES,min}^i < SoC_{BES}^i < SoC_{BES,max}^i \end{cases} \tag{5}$$

Where $E_{BES,cap}^i$ is the maximum battery capacity, $SoC_{BES,min}^i$ and $SoC_{BES,max}^i$ are the minimum and maximum SoC of the battery and are set to 20 % and 80 % respectively to avoid overcharging and deep discharging of the battery.

3) Electric vehicle modelling: The EV acts as a domestic battery storage and provides back-up power to supply the home appliances during short-term outages or during peak demand when electricity prices are higher. EV owners can participate in the P2P market by selling energy to other customers. With Vehicle-to-Home (V2H) technology, the EV becomes part of the smart home, and its charging-discharging operations are supervised by the HEMS. The energy stored in the EV battery during the availability time of the EV at home is given by:

$$E_{EV}^i(t) = H_j^i(EV) \Big[E_{EV}^i(t-1)\big(1 - \delta_{SD,EV}^i\big) +$$

$$U_{EV}^i P_{EV,ch}^i(t) \mu_{EV,ch}^i - \frac{(1-U_{EV}^i)P_{EV,dis}^i(t)}{\mu_{EV,dis}^i} \Big] \tag{6}$$

$$P_{EV,ch}^i(t) = E_{EV,chfPV}^i(t) + E_{EV,bfG}^i(t) + E_{EV,bfP2P}^i(t), \forall t \in [T_a, T_d] \tag{7}$$

$$P_{EV,dis}^i(t) = E_{EV,tH}^i(t) + E_{EV,stG}^i(t) + E_{EV,stP2P}^i(t) , \forall t \in [T_a, T_d] \tag{8}$$

$H_j^i(EV)$ returns 1 if the household is equipped with EV and 0 otherwise. To avoid charging and discharging to occur at the same time, the availability of the EV for charging and discharging, denoted U_{EV}^i, is introduced and takes the value 1 when the EV is charging and 0 when it is discharging. Equation (7) represents the charging power of the EV battery which can come from the PV ($E_{EV,chfPV}^i(t)$), from the grid ($E_{EV,bfG}^i(t)$) or purchased from the P2P market ($E_{EV,bfP2P}^i(t)$). Equation (8) represents the discharging power of the battery to supply the
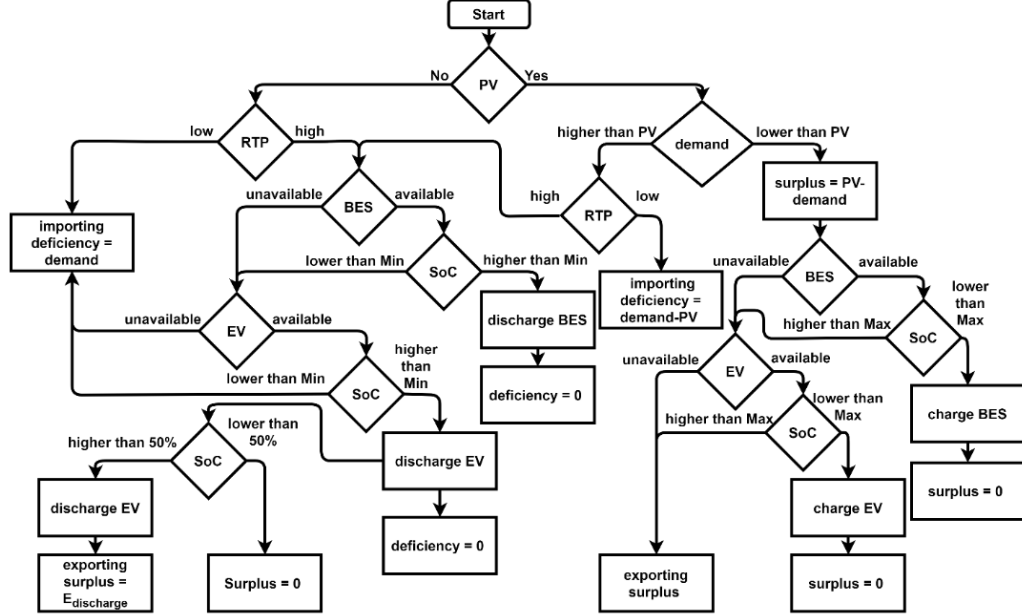
Fig. 2 Flowchart of the proposed HEMS.

home appliances $(E^i_{EV,tH}(t))$, to be exported to the grid $(E^i_{EV,stG}(t))$ or to be exported to the P2P market $(E^i_{EV,stP2P}(t))$. The availability time of the EV is limited between the EV's arrival time (T_a) to the house and the departure time (T_d). The SoC of the EV battery, with its charging and discharging limits is given by:

$$\begin{cases} SoC^i_{EV} = \dfrac{E^i_{EV}(t)}{E^i_{EV,cap}} \times 100\% \\ SoC^i_{EV,min} < SoC^i_{EV} < SoC^i_{EV,max} \end{cases} \quad (9)$$

The energy consumed during each trip is calculated as:

$$E^i_{EV,trip} = \frac{D_{trip}}{D_{max}} \times E^i_{EV,cap} \quad (10)$$

Where D_{trip} and D_{max} represent the trip distance and the maximum distance the EV can travel when the battery is fully charged, respectively, $E^i_{EV,cap}$ denotes the maximum energy capacity of the EV battery.

4) *Modelling of the net energy:* Solar PV generation can be used to power the household appliances, charge the home BES and the EV battery. The extra power, if any, can be either sold to the P2P market and/or the main grid. Note that the home BES can only supply the household load and charge only from the PV when possible. The EV battery, on the other hand, can be charged from the PV, from the P2P market or the main grid and it can supply the household appliances and sell energy to the P2P market or the main grid. The net energy of household i is the difference between the energy supply and demand at each time slot.

$$E^i_{net}(t) = E^i_{demand}(t) - E^i_{supply}(t), \forall t \in [0,T] \quad (11)$$

$$E^i_{demand}(t) = E^i_L(t) + U^i_{BES}P^i_{BES,ch}(t) + U^i_{EV}P^i_{EV,ch}(t), \forall t \in [0,T] \quad (12)$$

$$E^i_{supply}(t) = E^i_{PV}(t) + (1 - U^i_{BES})P^i_{BES,dis}(t) + (1 - U^i_{EV})P^i_{EV,dis}(t), \forall t[0,T] \quad (13)$$

If $E^i_{net}(t) < 0$, the surplus power the customer can sell is:

$$E^i_{surplus}(t) = -\left|E^i_{net}(t)\right|, \forall t \in [0,T] \quad (14)$$

If $E^i_{net}(t) > 0$, the deficiency power the customer needs to buy is:

$$E^i_{deficiency}(t) = \left|E^i_{net}(t)\right|, \forall t \in [0,T] \quad (15)$$

C. Home Energy Management System

With HEMS, the user can monitor, control, and optimize the amount of energy generated and consumed in real time, based on the customer's preferences via a dedicated user interface. This enables users to actively participate in the P2P market. Thus, the HEMS should be designed to accommodate different types of household resources such as local generation from renewable energy sources (RES), BES and EV. The flowchart of Fig. 2 describes the proposed HEMS. Generally, PV generation, when available, is first used to supply the household appliances. When the PV generation is higher than the household demand, the surplus of energy will be first stored in the batteries (BES or EV batteries), and the remaining will be sold to other peers in the microgrid. If the PV generation is lower than the household demand, the difference will be purchased from the P2P market if the energy price is low or provided from the batteries otherwise. However, when there is no PV generation, the required power for the household will be purchased from the P2P market if the price is low or taken from the batteries if the price in the P2P market is higher.

D. Consideration of physical network constrains

Although the P2P energy sharing benefits both peers and the main grid, technical challenges such as voltage stability and overflow in the physical layer arise with the implementation of a P2P market with the absent of control and management process in the P2P trading. Therefore, the physical network

constrains must be considered to avoid the violation of voltage and capacity issues. In this paper, the proposed P2P trading mechanism is also proposed with taking in the account of the physical network constrains.

Consider a radial distribution network that consists of a set $\mathcal{N}$ of buses and a set $\mathcal{E}$ of distribution lines connecting these buses. We index the buses in $\mathcal{N}$ by $i = 0,1,2, \dots n$, and denote a line in $\mathcal{E}$ by the pair (i,j) of buses it connects and the index i denotes the bus that is closer to the feeder. Bus 0 denotes the feeder, which has fixed voltage but flexible power injection to balance the loads. For each link $(i,j) \in \mathcal{E}$, let $z_{ij} = r_{ij} + ix_{ij}$ be the impedance on line (i,j), and $S_{i,j} = P_{i,j} + iQ_{i,j}$ and $I_{i,j}$ the complex power and current flowing from bus i to bus j. At each bus $i \in \mathcal{N}$, let $s_i = p_i + iq_i$ be the complex load and V_i the complex voltage. As customary, we assume that the complex voltage V_0 on the feeder is given and fixed. The branch flow model, proposed in [20], models power flows in a steady state in a radial distribution network: for each $(i,j) \in \mathcal{E}$,

$$\frac{P_{i,j}^2 + Q_{i,j}^2}{v_i} = \ell_{i,j} \qquad (16)$$

$$P_{i,j} = r_{i,j}\ell_{i,j} + p_j + \sum_{h:(j,k)\in\mathcal{E}} P_{j,k} \qquad (17)$$

$$Q_{i,j} = x_{i,j}\ell_{i,j} + q_j + \sum_{h:(j,k)\in\mathcal{E}} Q_{j,k} \qquad (18)$$

$$v_i - v_j = 2(r_{i,j}P_{i,j} + x_{i,j}Q_{i,j}) - (r_{i,j}^2 + x_{i,j}^2)\ell_{i,j} \qquad (19)$$

Subject to:

$$v_i^{min} \le v_i \le v_i^{max}, i = 1, \dots, n \qquad (20)$$

$$p_i^{min} \le p_i \le p_i^{max}, i = 1, \dots, n \qquad (21)$$

$$q_i^{min} \le q_i \le q_i^{max}, i = 1, \dots, n \qquad (22)$$

Where $\ell_{i,j} = |I_{i,j}|^2$, $v_i = |V_i|^2$. It is worth noting that the net reactive power for each bus must thus be calculated for each time step t. For simplicity, it was decided to find an average power factor for each of the buses and keep it constant for all time steps. From the given network data, it was obtained that all buses maintained a constant power factor of 0.98. The reactive power for each house i for each time step t was thus calculated with:

$$q_i = \sqrt{\frac{p_i^2}{cos\theta^2} - p_i^2} = \sqrt{\frac{p_i^2}{0.98^2} - p_i^2}, \forall i \in \mathcal{E} \qquad (23)$$

To ensure that the P2P mechanism does not violate the physical constrains (equations 38-40), every time the Energy sharing Coordinator (ECS) receives the selling/buying request from prosumers/consumers, voltage variation and line
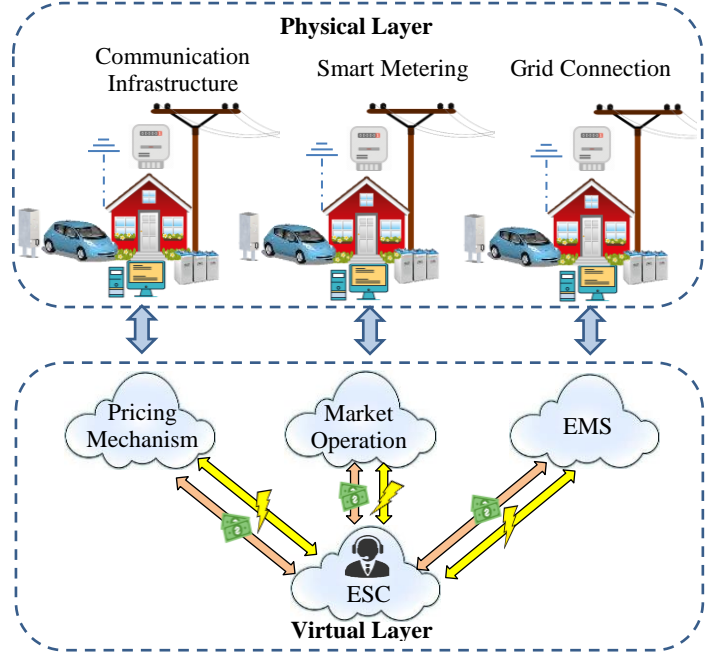

Fig. 3 P2P energy sharing structure.

congestion are evaluated. And then all participants receive a signal which informs them if they can still participate in the market without causing problems in the network. For example, one prosumer could reduce the injected power into the grid at a certain time due to the high risk of causing voltage problems in the network.

III. P2P ENERGY SHARING MODEL

A. P2P Energy Sharing Structure

For the P2P energy trading structure of the community microgrid, it is assumed that all participants are connected to one another through the bidirectional energy and information flows, and the whole community is linked to the utility grid via a network connection point. Based on this structure, the peers can trade their excess energy among themselves, instead of directly trading with the utility grid. As shown in Fig.3, the P2P sharing system is assumed to have two layers: a physical layer and a virtual layer. The physical layer is responsible for the physical connection and transfer of energy between prosumers within the community through a local distribution network. In addition, it is assumed that all houses are equipped with smart meters to collect data such as PV generation, energy consumption, state-of-charge (SOC) of the ESS and EV, and energy transactions with P2P market or with the utility grid. Moreover, the communication network is used to enable the smart meter to exchange the data.

The virtual layer provides a secure network environment for all the peers to have equal access to the P2P market. In the virtual layer, it is assumed that each participant is equipped with an Energy management System (EMS), which is responsible for managing the energy flow within the household and energy import/export on behalf of the consumer/prosumer. As shown in Fig.3, both the trading process and the communication of information are done in a centralized fashion via an ESC who

can communicate with each peer within the community. The ESC manages energy transactions, price mechanism, purchase, and sale expenses settlement, and interacts with the utility grid considering the physical network constrains to avoid the violation of voltage and capacity issues. Peers, on the other hand, will pay/gain their energy cost/revenue based on the amount of energy imported/exported using the predefined pricing mechanism. It is worth noting that this paper focuses only on the application of energy trading in the virtual layer of the P2P energy sharing model.

B. P2P Energy Sharing Mechanism

The P2P energy trading mechanism is designed to motivate residents to participate in the energy market. The basic principle of economics states that the goods price increases when the demand increases and the production decreases, and vice versa. In this paper, a new P2P pricing mechanism is proposed to ensure all customers in a community make economic benefits, in other words they will be better off compared to the traditional utility grid market. The proposed pricing mechanism can be applied to any P2P energy sharing model. The proposed mechanism does not consider only the relationship of the surplus and deficiency of power, but also considers the RTP of the power grid and FiT which reflect the demand of the power system, where the price is high during peak demand and lower during off-demand. Then demand response (DR) program is implemented to encourage consumers to manage their energy consumption, to reduce the stress on the power grid and ensure that energy exchange among the peers does not violate network constraints. The proposed P2P model assumes that (i) the internal selling and buying prices are bounded between the FiT and RTP prices and (ii) the buying price is higher than selling price except in the case where the energy deficiency equals the energy surplus, in which case the buying and selling prices are equal.

For each time slot, the total energy surplus exported to the P2P market by n prosumers is defined as:

$$E_S(t) = \sum_{i=1}^{n} E_{surplus}^i(t), \forall t \in [0, T] \qquad (24)$$

The total energy deficiency purchased by m consumers is defined as:

$$E_D(t) = \sum_{i=1}^{m} E_{deficiency}^i(t), \forall t \in [0, T] \qquad (25)$$

Since the P2P prices depend on the relationship between the energy deficiency and energy surplus that need to be traded at the P2P market, this measure is defined by the α-ratio given by:

$$\alpha = \frac{E_D - E_S}{E_D + E_S} \qquad , \alpha \in [-1, 1] \qquad (26)$$

When $\alpha = 0$, the surplus equals the deficiency ($E_S(t) = E_D(t)$) as shown in Fig.4, when $\alpha \approx -1$, there is no deficiency ($E_D(t) = 0$) or the surplus is much larger than the deficiency ($E_S(t) \gg E_D(t)$) and when $\alpha \approx 1$, there is no surplus exported or the surplus is much smaller than the deficiency ($E_S(t) \ll E_D(t)$).

The energy price of the main grid fluctuates during the day; it is higher during peak demand periods and lower during off-
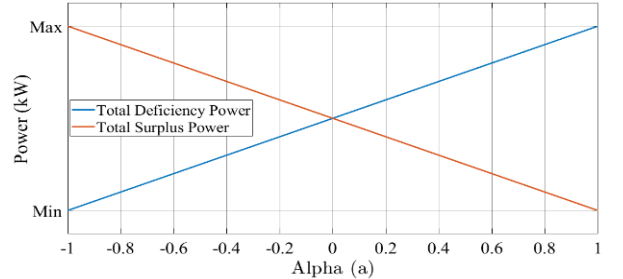

Fig. 4 Different values of alpha α and among different values of surplus power $E_S(t)$ and deficiency power $E_D(t)$.

peak periods which affects the internal P2P prices.

Therefore, the relationship between the import and FiT prices can be expressed as:

$$\beta = \frac{r_{ex}}{r_{ex} + r_g} \quad , r_{ex} < r_g \qquad (27)$$

Where r_g is the RTP of the main grid and r_{ex} is the FiT.

Therefore, the P2P market price is calculated based on (α) and (β) parameters as:

$$r_b = \begin{cases} \left(\frac{r_g - r_{ex}}{2}\right) \frac{(2-\beta)e^{2\alpha} + \beta e^{-2\alpha}}{e^{2\alpha} + e^{-2\alpha}} + r_{ex} & , \alpha \geq 0 \\ \left(\frac{r_g - r_{ex}}{2}\right) \frac{(1+\beta)e^{2\alpha} + (1-\beta)e^{-2\alpha}}{e^{2\alpha} + e^{-2\alpha}} + r_{ex} & , \alpha < 0 \\ r_g & , E_S(t) = 0 \end{cases} \qquad (28)$$

$$r_s = \begin{cases} \left(\frac{r_g - r_{ex}}{2}\right) \frac{(1+\beta)e^{2\alpha} + (1-\beta)e^{-2\alpha}}{e^{2\alpha} + e^{-2\alpha}} + r_{ex} & , \alpha \geq 0 \\ \left(\frac{r_g - r_{ex}}{2}\right) \frac{(2-\beta)e^{2\alpha} + \beta e^{-2\alpha}}{e^{2\alpha} + e^{-2\alpha}} + r_{ex} & , \alpha < 0 \\ r_{ex} & , E_D(t) = 0 \end{cases} \qquad (29)$$

Fig. 5 shows the P2P market prices under the proposed price mechanism with three different values of RTP as FiT is constant

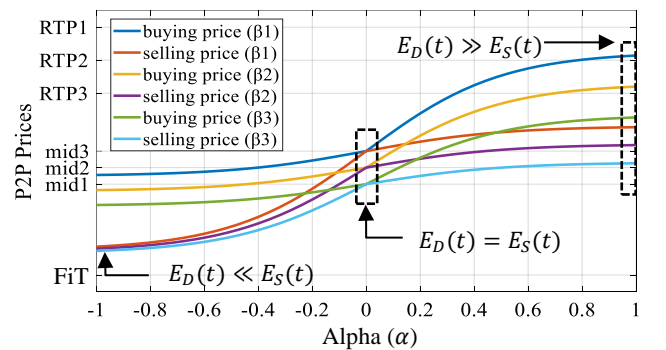
Fig. 5 P2P market prices under the proposed price mechanism with different values of α and β.

throughout the day.

The main features of this price mechanism are: (i) The P2P market prices are bounded between the RTP and FiT. (ii) When $E_D(t) = E_S(t)$, the P2P prices are set to the Mid-Rate Ratio (MMR), which refers to the mean value of the RTP and FiT prices. (iii) P2P buying price is always higher than P2P selling price. (iv) P2P market prices are higher than MMR when $E_D(t) > E_S(t)$, $\alpha > 0$. (v) P2P market prices are lower than

MMR when $E_D(t) < E_S(t)$, $\alpha < 0$. (vi) With increasing RTP, the P2P market prices increase based on β value, and vice versa.

C. Cost Function

The role of the ESC is to supervise the transactions in the P2P market. His main responsibilities are to set the trading rules and manage the trading activities, as well as supervise the metering, billing, and information sharing. After receiving a bid from a prosumer, the ESC runs the pricing model to obtain P2P prices based on the deficiency-surplus ratio, and RTP-FiT prices. At each time slot, the individual energy cost for each participant is calculated using Algorithm 1 given in Table 1. During the operation, the following possible cases could occur at each time step:

1. $E_D(t) > 0$ and $E_S(t) = 0$: When the ESC receives only the energy deficiency requests from consumers, he will buy energy from the main grid to meet the demand and the individual energy cost for each consumer i is defined as in line (8) of Algorithm 1.

2. $E_S(t) > 0$ and $E_D(t) = 0$: In this case, there is no energy deficiency request from consumers, thus the amount of energy surplus will be exported to the main grid under FiT price and the individual cost is calculated using line (11) of Algorithm 1.

3. $E_D(t) > E_S(t)$, $E_S(t) \neq 0$: When the amount of deficiency is higher than the surplus, then the ESC needs to buy energy from the main grid to meet the energy deficiency. In this case, lines (12-21) are implemented. Firstly, the amount of energy purchased from the grid is defined using line (13). Consequently, calculating the individual energy cost depends on whether the participant is buying or selling energy. Lines (16) and (17) calculate respectively the cost of the energy purchased from P2P market and main grid, and then the total individual cost is determined using line (18). For users who are selling energy, the profit is calculated using line (20).

4. $E_S(t) > E_D(t)$, $E_D(t) \neq 0$: In this case, the total energy surplus is greater than the total deficiency. Therefore, the extra energy will be sold to the main grid. The individual energy cost is calculated with lines (22-31).

5. Firstly, the amount of energy sold to the main grid is determined using line (23), then the energy cost is calculated using line (28) which is the sum of the cost from selling energy to consumers (line 26) and the main grid (line 27). The individual energy cost for users who are buying energy from the P2P market is calculated with line (30).

6. $E_S(t) = E_D(t)$: When the total surplus meets the deficiency, the P2P selling and buying prices are equal. The energy cost for prosumers and consumers are calculated using lines (35) and (37) respectively.

IV. SIMULATION RESULTS AND DISCUSSION

A. Simulation Setup

In this paper, the uncertainties in the load demand of the houses, the PV generation, and the flexibility of EVs are simulated using the MCS which produces 1000 scenarios of possible probabilities. A suitable distribution function has been

TABLE 1 Proposed cost function.

Algorithm 1
1: **For** t = 1 to 24
2:   Read RTP (r_g) and FiT (r_{ex}), number of households (N)
3:   Receive E_D and E_S requests
4:   Implement pricing model to specify r_b and r_s
5:   **For** i =1 to N
6:     **if** $E_D(t) > 0$ and $E_S(t) = 0$
7:       Calculate individual energy cost as:
8:       $C^i(t) = E^i_{deficiency}(t) * r_g$
9:     **elseif** $E_S(t) > 0$ and $E_D(t) = 0$
10:       Calculate individual energy cost as:
11:       $C^i(t) = E^i_{surplus}(t) * r_{ex}$
12:     **elseif** $E_D(t) > E_S(t)$ and $E_S(t) \neq 0$
13:       $E_{bfg}(t) = E_D(t) - E_S(t)$
14:       Calculate individual energy cost as:
15:       **if** $E^i_{deficiency}(t) > 0$
16:         $c^i_{bfP2P}(t) = \frac{E^i_{deficiency}(t)*E_S(t)*r_b}{E_D(t)}$
17:         $c^i_{bfg}(t) = \frac{E^i_{deficiency}(t)*E_{bfg}(t)*r_g}{E_D(t)}$
18:         $C^i(t) = c^i_{bfP2P}(t) + c^i_{bfg}$
19:       **elseif** $E^i_{surplus}(t) > 0$
20:         $C^i(t) = E^i_{surplus}(t) * r_s$
21:       **endif**
22:     **elseif** $E_S(t) > E_D(t)$ and $E_D(t) \neq 0$
23:       $E_{stg}(t) = E_S(t) - E_D(t)$
24:       Calculate individual cost as:
25:       **if** $E^i_{surplus}(t) > 0$
26:         $c^i_{stP2P}(t) = \frac{E^i_{surplus}(t)*E_D(t)*r_s}{E_S(t)}$
27:         $c^i_{stg}(t) = \frac{E^i_{surplus}(t)*E_{stg}(t)*r_{ex}}{E_D(t)}$
28:         $C^i(t) = c^i_{stP2P}(t) + c^i_{stg}(t)$
29:       **elseif** $E^i_{deficiency}(t) > 0$
30:         $C^i(t) = E^i_{deficiency}(t) * r_b$
31:       **endif**
32:     **elseif** $E_S(t) = E_D(t)$
33:       Calculate individual cost as:
34:       **if** $E^i_{surplus}(t) > 0$
35:         $C^i(t) = E^i_{surplus}(t) * r_s$
36:       **elseif** $E^i_{deficiency}(t) > 0$
37:         $C^i(t) = E^i_{deficiency}(t) * r_b$
38:       **endif**
39:     **endif**
40:   **end**
41: **end**

TABLE 2 Types of households

Household Type	PV	BES	EV	Probability Density
1	Yes	Yes	Yes	0.07
2	Yes	Yes	No	0.1
3	Yes	No	Yes	0.1
4	Yes	No	No	0.18
5	No	No	Yes	0.15
6	No	No	No	0.4

assigned to each parameter of the load demand, PV generation and EVs. Then the input data for the MCS is extracted from the Probability Density Function (PDF) generated by these distribution functions.

1) household demands

To address the uncertainty of the household demand, the residential area with 100 households is firstly classified into six types $[H_1, H_2, H_3, H_4, H_5, H_6]$ based on the type of household

they own. The number of each type of these houses is extracted from the weighted uniform distribution as shown in Table 2.

The daily household load depends on the house's size and profile class as presented in Ofgem (UK's energy regulator) report [21]. According to this report, a typical household loads divided into two profiles. Profile 1 is domestic unrestricted, which most homes fall under (60%). While Profile 2 (40%) covers Domestic Economy 7, where users have a lower off-peak rate at night, when they pay less for their electricity as shown in Table 3. The probability density of the household size is based on the real data extracted from [22] which presents the number of household size by number of bedrooms in England/London, 2011. Fig. 6 shows the weights of the uniform distribution function of each household size based on the number of bedrooms.

TABLE 3 TYPICAL HOUSEHOLD'S ENERGY USAGE IN UK

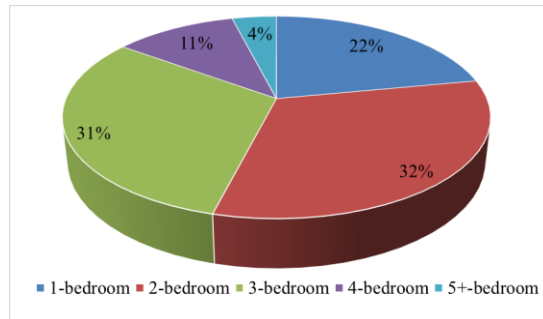| Household Size	Electricity Consumption (kWh)			
	Profile Class 1		Profile Class 2	
	Annual	Daily	Annual	Daily
1–2-bedroom household/flat	1,800	5	2,400	6.7
3–4-bedroom house	2,900	8	4,200	11.7
5+ bedroom house	4,300	12	7,100	19.7

Fig. 6 Distribution of household size by number of bedrooms.

Generally, peak electricity consumption occurs during morning hours [7:00 am-12:00 pm] when the household occupants wake up and during the evening [16:00 pm -21:00 pm] when the occupants start cooking, watching TV and doing other activities. Off-peak hours usually correspond to the period from mid-night till the morning.

2) Probability distribution for stochastic parameters of EVs

The availability of EVs depends on several factors, such as the EV owners' travelling patterns and usage, EVs' type, the capacities of their batteries, and the arrival and departure times. Therefore, it is essential to develop a comprehensive model to determine the availability of EVs. In this paper, the distribution functions are used to create the PDF of all the parameters and variables for each EV to be used as an input to the MCS to produce different scenarios.

a) EVs classification

In the UK, individual EVs based on their size and use are classified into the following four basic categories [23]:

- L7e: Quadricycle-four wheels, with a maximum unladen mass of 400 kg or 550 kg for goods carrying vehicles.

- M1: Passenger vehicle, four wheels up to 8 seats in addition to the driver's seat.
- N1: Goods-carrying vehicle, four wheels, with a maximum laden mass of 3500 kg.
- N2: Goods-carrying vehicle, four wheels, with a maximum laden mass between 3500 kg and 12,000 kg.

The real data presented in [23] regarding the number of the above four types of EVs in the UK in 2020 is used to create a
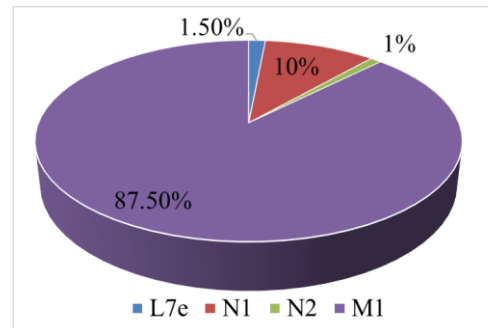

Fig. 7 Distribution of EVs categories.

weighted uniform distribution function. Fig. 7 shows the PDF used to determine the category of each EV.

b) Departure and arrival times

It is assumed that the peak-hour of departure time of EVs is 8:00 am as people start leaving their premises, while the peak - hour of arrival time is 18:00 pm as users return home. To address the uncertainties, Departure and arrival times are assumed to have a Weilbull distribution with scale and shape parameters as shown Fig. 8 (a) and Fig.8 (b), respectively.
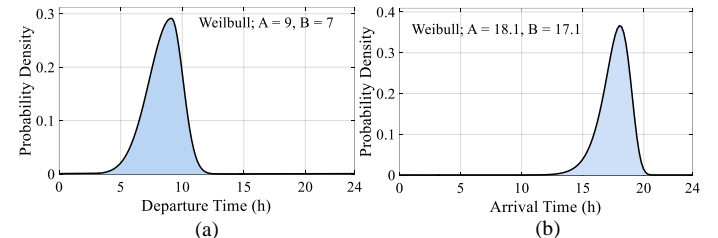

Fig. 8 Probability density of departure and arrival times.

c) Battery characteristics and daily travelling distance

The random values for the rated battery capacity for each type of EV are generated based on the Gamma and Normal distributions to create the most suitable probability density functions [23]. Fig. 9 shows the PDFs of the battery capacities for each EV's category. For example, the Gamma distribution with shape set to 10.8 and scale set to 0.8 is used for L7e category and the battery capacity is bounded between 5 and 15 kWh.

According to the statistical data set published by the Department of Transport in England 2020 [24], the distribution of daily distance is fitted as a normal distribution with the average value set to 39.9 km and the deviation set to 10 km to create the PDF of EV travelling distance as shown in Fig. 10.

To specify the initial amount of EV's SoC, it is essential to determine the energy consumption per kilometer. To this end, the distributions of EV energy consumption per kilometer for
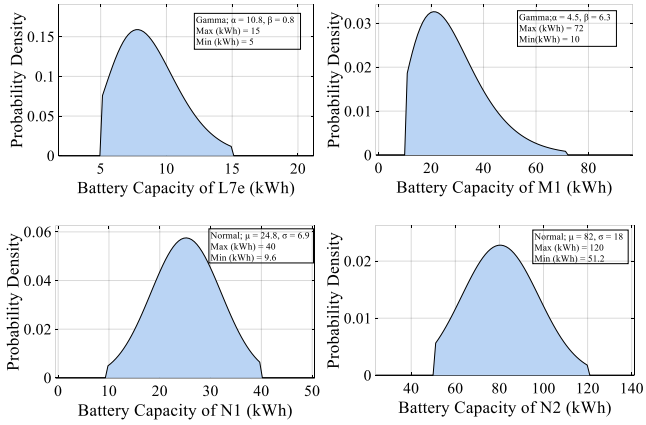
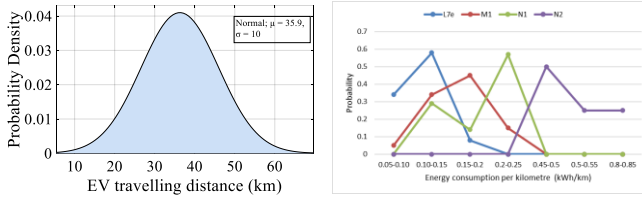Fig. 9 Probability of battery capacity of EVs' categories.

Fig. 10 probability of EV travelling distance.

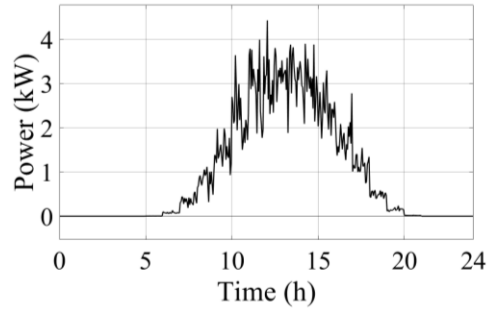Fig. 11 Probability of energy consumption of each EV category.

Fig. 12 Stochastic PV generation.

The key function of the HEMS is to provide energy management services to minimise the power consumption in the smart home. This functionality includes monitoring, control and management of renewable energy generation, energy storage, and energy consumption. HEMS also receives price signals from the utility grid and the P2P market and performs demand response analysis. To investigate the performance of the proposed HEMS to satisfy the household demand, one scenario that has the highest probabilities of MCS is selected to illustrate the power profiles of the six households' types. In Table 4, the details for this scenario are listed of each household.

all types of EVs are shown in Fig. 11 [23].

d)   Initial SoC and target SoC of EVs

To satisfy the charging demand for each EV, the target SoC of each EV is selected randomly using the uniform distribution [65%, 80%]. Based on the target SoC, the travelling distance and energy consumption per kilometer values, the initial SoC for each EV can then be calculated as:

$$SoC_{initial}^{i} = \varphi^{i} \cdot \left(SoC_{target}^{i} - \frac{C_{kWh/km}^{i} \times D_{trip}^{i}}{E_{EV,cap}^{i}} \right) \quad (30)$$

$C_{kWh/km}^{i}$ is the energy consumption per kilometer. φ^{i} is an energy efficiency coefficient which is used to consider the energy loss brought by the speed change process, and it varies uniformly in the range of [0.9,1.0].

3)   Probability distribution for stochastic parameters of PV

As the PV power generation is highly uncertain due to variations in the solar irradiance level throughout different hours of the day. Hence, the modelling of PV uncertainty can be addressed either directly as a PDF of the PV power yield or indirectly as a PDF related to the solar irradiance which is subsequently fed into a PV system model. In this paper, A stochastic model of PV production is built based on the adopted historical solar irradiance data extracted from [25] with zero mean and standard deviation of 15%. Fig.12 shows one of the random scenarios of power generation of the PV.

B.   Evaluation of the proposed HEMS

1)   Impact HEMS on individual household demand

In this study, it is assumed that all participants in the P2P energy sharing are equipped with a HEMS in their households.

TABLE 4 Details of the six test houses.

House type	House load (kWh)	PV (kWh)	BES		EV Battery	
			Cap. (kWh)	Initial SoC (%)	Cap. (kWh)	Initial SoC (%)
H_1	19.7	4	5	40	50	39
H_2	8	3	6	35	-	-
H_3	12	3	-	-	40	37
H_4	8	3	-	-	-	-
H_5	12	-	-	-	60	42
H_6	5	-	-	-	-	-

"-" = not applicable, "cap." = Capacity.

By using the proposed HEMS algorithm of Fig. 2, the energy consumption profiles of the selected six households throughout the day are shown in Fig. 13. Household Type 1 (H_1) is equipped with PV, BES and EV as shown in Table 4. It can be noted that, during the time interval [12:00 am – 6:00 am], the HEMS sends a request of energy deficiency to the ESC as there is no PV generation, the energy demand and the electricity price are lower as shown in Fig.13(a). At 6:00 am, the price is high, then the BES starts discharging to supply the household demand, until there is no deficiency energy. During [7:00 am – 9:00 am], the solar PV starts generating. Therefore, the household load is supplied from the PV and the surplus is used to charge the BES. Once the BES reaches the maximum SoC, the remaining power is exported to the P2P market. This occurs during the time [9:00 am- 13:00 pm]. Once the EV returns home, and there is still PV generation, the surplus of power is used to charge the EV battery till the SoC reaches 80 %. Then the surplus of power is fed back to the P2P market again. During the time [16:00 pm-18:00 pm], the household load reaches the
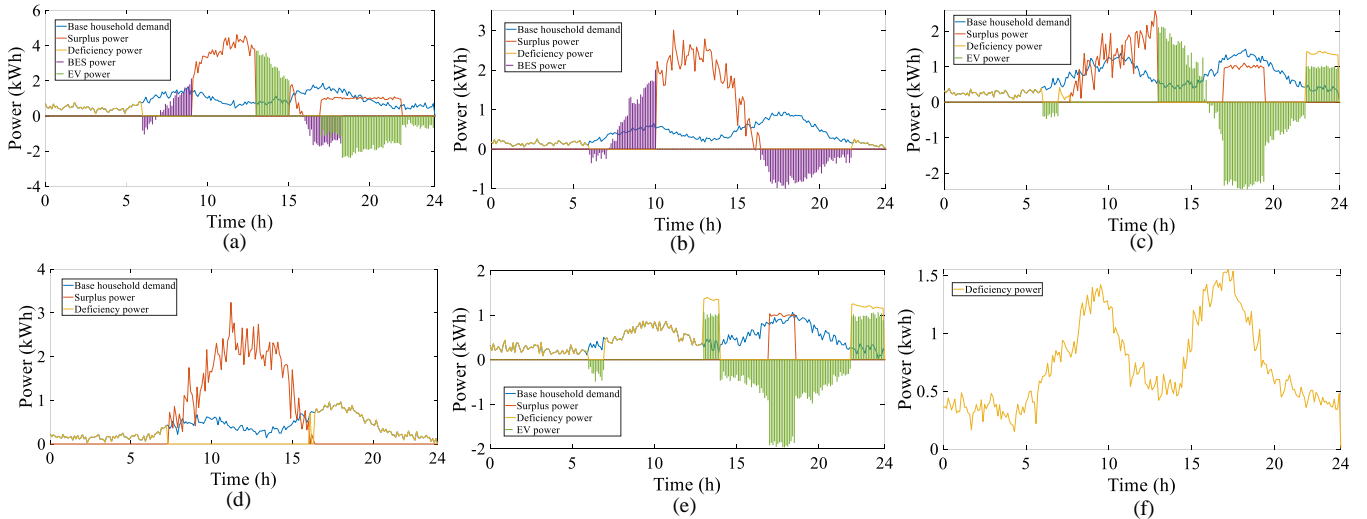
Fig. 13 Random scenario of the power profiles for the six household types throughout the day under the proposed HEMS.

peak value, thus the BES is used to supply the household appliances. The EV battery is discharging to sell energy to the P2P market during [17:00 pm- 18:00 pm], as the SoC of the EV is at its full capacity, and the electricity price is also high. From 18:00 pm to 22:00 pm, the EV is selling energy to the P2P market and supplying energy to the household load.

Household Type 2 (H_2) sends energy deficiency request to the P2P market during [12:00 am- 6:00 am] and [22:00 pm – 12:00 am] and exports the surplus energy during [10:00 am – 16:00 pm] as shown in Fig.13(b). Since this household type is equipped with PV and BES, the BES charges from the surplus of PV and then is used later to supply the household load during the evening peak demand.

For household Type 3 (H_3), the energy deficiency request is sent to the P2P market during early morning time [12:00 am- 6:00 am] to supply the household appliances as there is no PV generation and the electricity price is lower. At 6:00 am, the electricity price becomes higher, hence it is better to use the EV battery to supply the household appliances. Since this household is not equipped with BES, the surplus energy request is sent to the P2P market during the PV generation [7:00 am- 13:00 pm]. Once the EV returns home at 13:00 pm, the surplus power is used to charge EV battery. During [16:00 pm-22:00 am], the household load is powered by discharging the EV battery. From 16:30 pm to 19:30 pm, the EV is utilized to sell energy to P2P market as there is enough SoC and the electricity price is high shown in Fig.13(c).

The load curve of household Type 4 (H_4) is presented in Fig.13(d), This household is equipped with solar PV only. Therefore, the surplus of energy can be sold only to the P2P market. When there is no PV generation, the user buys the required energy from the P2P market.

As Household Type 5 (H_5) owns only an EV, the household load is supplied by importing energy from the P2P market most of the time as shown in Fig. 13(e). The EV battery is charged only during off-peak periods because energy prices are lower. While the surplus of energy is exported to the P2P market during [16:30 pm-18:00 pm] by discharging the EV battery.

(a) Deficit and surplus power of Household Type 1.

(b) Deficit and surplus power of Household Type 2.

(c) Deficit and surplus power of Household Type 3.

(d) Deficit and surplus power of Household Type 4.

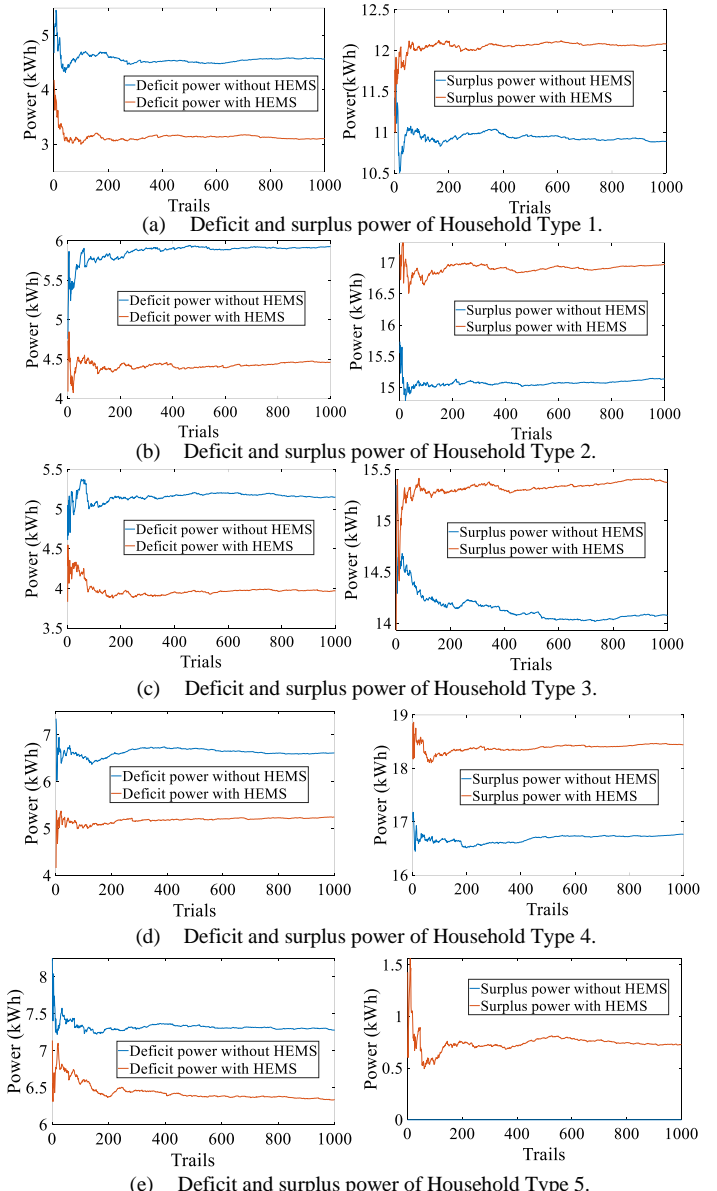(e) Deficit and surplus power of Household Type 5.

Fig. 14 Average amount of deficit/surplus for each group of households under 1000 scenarios of MCS.

The evening peak demand is covered with the energy stored in the EV battery due to the higher electricity price.

Household Type 6 (H_6) is considered as consumer all the time; hence his load is supplied by purchasing the required power from the P2P market as shown in Fig.13(f).

To evaluate the overall performance of the proposed HEMS within the community, the average amount of deficit/surplus for each group of households that belongs to same type has been calculated over 1000 scenarios of MCS with and without implementing HEMS and presented in Fig.14. Clearly, the proposed HEMS can effectively manage the energy flow within each type of household and simultaneously enable the EVs to participate in P2P market. For example, for households of Type 1, the average energy deficit has decreased using HEMS from 4.6 kWh to 3.2 kWh, while the surplus energy exported to the P2P market has increased using HEMS from 10.9 kWh to 12.1 kWh as shown in Fig.14 (a) and Fig.14 (b), respectively.

1) Impacts HEMS on microgrid

In microgrids, self-consumption of energy from renewable sources, such as photovoltaic panels, results in immediate positive impacts such as reduction in energy losses and mitigation of congestion problems in the distribution network. The self-consumption rate (SCR) (the amount of energy locally generated and consumed with respect to the total local generation) is considered as a performance measure to assess a microgrid's ability to consume its own locally generated energy. Consequently, maximizing the self-consumption rate is an implicit goal in most microgrid settings. To this end, the self-consumption of each type of households is evaluated to validate the proposed HEMS.
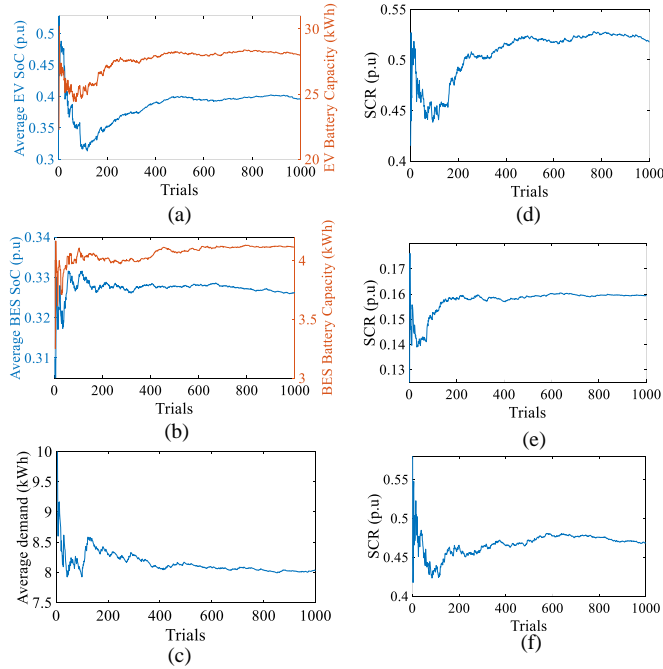

Fig. 15 Average values of 1000 scenarios of (a) EVs' capacities and SoCs, (b) BESs' capacities and SoCs, (c) household demand, (d) SCR of Type 1, (e) SCR of Type 2, and (f) SCR of Type 3.

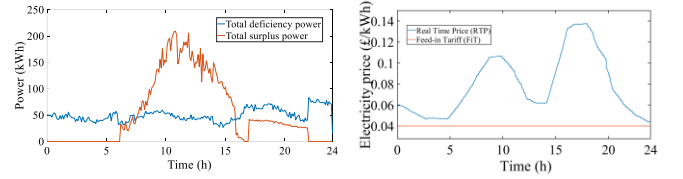As the battery energy storage plays a key role in increasing

Fig. 16 Surplus and deficiency power throughout a day.

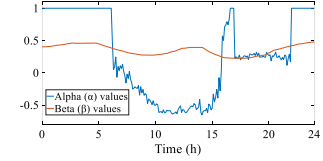Fig. 17 Real time price (RTP) and feed-in tariff (FiT).

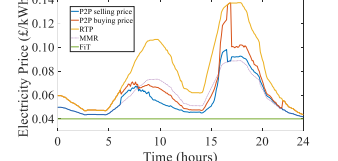Fig. 18 Alpha (α) and Beta (β) values.

Fig. 19 Internal P2P prices (buying and selling prices) under the proposed mechanism.

the self-consumption rate by storing the excess of energy generated by PVs to be used later when needed. For this reason, the impact of different SoCs and capacities of BES and/or EVs on the SCR is analysed for the households of Types 1, Type 2 and Type 3, which have BES and/or EV as shown in Fig. 15. Fig.15 (a) and Fig.15 (b) show the average initial SoCs and capacities of the EVs' and BESs' batteries respectively throughout the 1000 scenarios of the MCS. Fig.15 (c) shows the average daily load demand of the households in the community (8.01 kWh). As the households that belong to Type 1 have both EV and BES, these households have the highest SCR (52.5 %) as shown in Fig. 15(d). It is noted that how the lower battery capacity of the EVs influenced the SCR in the first 200 iterations. Fig.15 (e) shows the SCR of the households belong to Type 2, as this type of households has only BESs with the small average battery capacity (4.2 kWh), the SCR is 15.9%, while the households Type 3 has 47.3% of SCR as shown in Fig.15 (f), since these households have only EVs. Therefore, the SCR depends mainly on the capacity of EV and BES batteries and their SoCs. The batteries with higher capacity and lower SoCs consume more energy when they are charged. Therefore, the higher capacity of batteries, the lower are the SoCs, and the higher self-consumption rate is.

C. Evaluation of the Proposed P2P Price Mechanism

One scenario with the highest possibilities is selected to evaluate dynamic performance of the proposed P2P price mechanism. To decide on the P2P market prices for each time slot, the ESC receives the total deficiency and surplus of energy in real-time from the 100 users as shown in Fig.16, and the dynamic electricity prices from the main power grid (RTP and FiT) as shown in Fig.17. Based on the total surplus and deficiency power, and the power grid prices, Equations (26) and (27) are used to determine the values of α and β. Fig.18 shows the variation of these parameters over one day period. Consequently, using equations (28) and (29), the P2P market buying and selling prices are decided as shown in Fig.19.

It is obvious that when $\alpha = 1$ (means there is no surplus of energy exported to the P2P market), the ESC purchases energy from the main power grid under the RTP. During [6:00 am-8:00 am], the energy deficiency is higher than the surplus of energy,
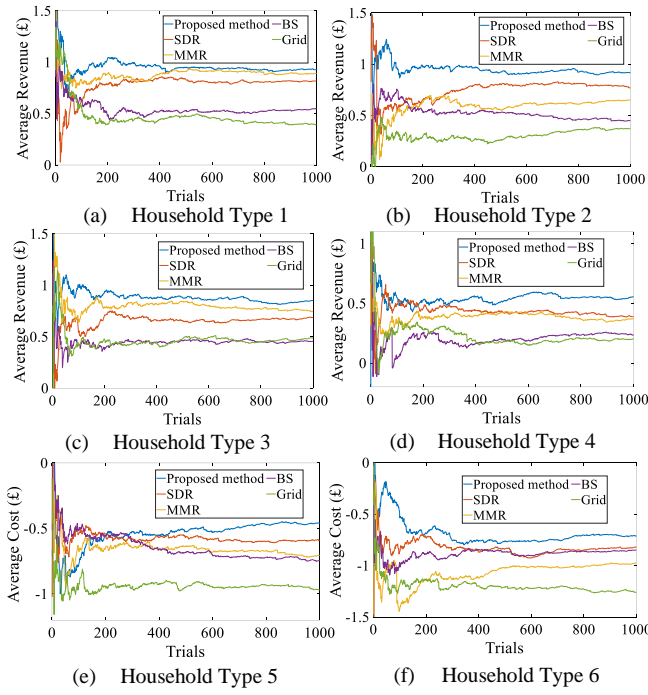
Fig. 20 Evaluation results of three existing P2P energy sharing models (SDR, MMR and BS) under 1000 scenarios of MCS.

hence the P2P trading prices are higher than the Mid-Market Rate (MMR) price. However, when the surplus of energy is higher than energy deficiency during [8:00 am- 16:00 pm], the P2P buying and selling prices are less than the MMR price.

1) Comparison with other P2P models

The performance of the proposed pricing mechanism has been compared with three existing P2P energy sharing mechanisms, namely, the Bill Sharing (BS), Mid-Market Rate and Supply-Demand Ratio (SDR). A detailed description and definition of these three mechanisms is provided in Appendix B. The three pricing mechanisms were simulated and evaluated under 1000 scenarios, and results of the MCS are presented in Fig.20 that contains the profits/cost of the six types of households within the community.

From Fig.20, it can be observed that the proposed pricing mechanism can fairly guarantee the highest profit/cost for all prosumers/consumers within the community compared to other mechanisms as shown in Fig.15 (a)-(f). In terms of the overall performance, the proposed mechanism preformed the best with 42.1% of improvement in the economy index of all participants in the community.

Although the SDR mechanism has a better overall performance (with 37.3% of the overall performance) for all participants than both the BS and MMR mechanisms, it does not address the unfairness issue among participants. The reason behind this is that, using SDR mechanism as discussed in Appendix B.3, the P2P selling and buying prices are set to the FiT price when the total amount of energy surplus exported to the P2P market is higher than the total amount of energy deficiency (SDR>1). This confirms why the energy profits rate for Type 1 and Type 3 households (prosumers) is lower compared to MMR mechanism.

As for the MMR mechanism, the P2P prices are set to the

average value of RTP and FiT without considering the amount of energy exported or imported by the participants as discussed in Appendix B.2. When the energy surplus exported to the P2P market is higher than the energy deficiency, the P2P prices under the MMR method are higher than the P2P buying and selling prices under the proposed mechanism and SDR. This conflicts with the basic principle of economics states that the goods price decreases when the production increases and the demand decreases, and vice versa. That is why the cost-saving rate for Type 5 and Type 6 (consumers) is lower under the MMR method compared to both proposed mechanism and SDR as shown in Fig.20 (e) and Fig.20 (f), respectively. As these households (Type 5 and Type 6) bought a large amount of energy with higher price compared to the buying price of the proposed mechanism during [8:00 am- 16:00 pm]. However, the overall performance of MMR mechanism is 29.6%.

For the BS mechanism, although its overall performance was more than the conventional paradigm (trading with main grid) with an overall performance of 21.7% for all participants, some of the participants under the BS mechanism received lower income than that under the trading with the grid. The reason was that in the BS mechanism, the cost of electricity for a community is shared among the customers based on individual customer's total energy consumption and export, so that the ones with larger contribution (with high surplus energy) were not remunerated fairly because their energy was sold to the P2P market at a price lower than FiT.

2) Impacts P2P market on microgrid

To investigate how the proposed HEMS and P2P market can smooth the electricity demand of the community, the same scenario (with higher probabilities) as that selected in Section B and C is used.

In this scenario, the amounts of power that need to be purchased by the residential area from the main grid under different cases are shown in Fig.21, where CS0 refers to the base case of the total demand of all households within the community, CS1 refers to the total households' demand after implementing HEMS and CS2 refers to the total demand of all households' demand when participating in P2P market.

According to Fig.21, the whole amount of deficit that needs to be purchased from the main grid under the three cases are the same during the time period [12:00 am-6:30 am]. That is because there is no surplus power traded in the P2P market. During the period [6:30 am – 7:30 am], the deficit of energy that was purchased from the grid under CS1 and CS2 are the same. However, this amount of power is lower than that under CS0. This is because the households that own batteries started to use them to supply their appliances due to higher electricity prices. Around 7:30 am under CS2, the households that have PVs started to export their surplus of energy to the P2P market. It is noted that the whole community can satisfy its energy demand and there is no need to purchase energy from the main grid during [7:30 am-15:30 pm] as the P2P market covers the whole community demand. In addition, by motivating EV owners to participate in the P2P market during evening peak demand [16:00 pm-22:00 pm], they sell energy by discharging their EVs batteries and generate more revenue.
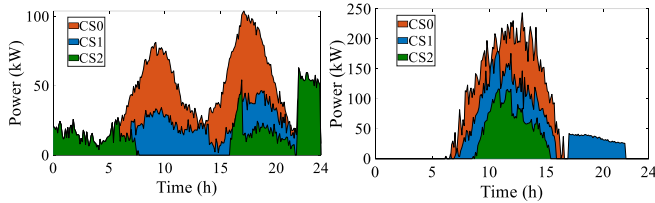
Fig. 21 Community demand that needs to be purchased from the main grid under different scenarios.

Fig. 22 Energy exported to the main grid under different scenarios.

Fig. 23 11-bus distribution system diagram.

On the other hand, the amount of energy surplus exported to the main grid by all households is decreased by 31% as a result of using the proposed HEMS (CS1) in every household as shown in Fig.22. The P2P trading (CS2) can contribute to a further reduction of the exported energy (up to 43%) by sharing energy within the community.

Overall, P2P trading enable better energy management by matching local demand and supply. Along with the higher local consumption of renewable energy, P2P electricity trading can help reduce investments related to the generation capacity and transmission infrastructure needed to meet peak demand.

3) Evaluation of P2P mechanism with considering physical network constrains

For the simulation, the 11-bus network that proposed in [26] has been analysed and modified. The network consists of the six types of households with the same probabilities as discussed in Section II.A. The distribution of the households within the network is shown in a Fig.23. It is assumed that the bus 1 is the slack bus where the ESC is located, who is responsible for preventing any network constraint violation. Therefore, the bus voltages do not violate the standard, which is ±5% of 1 per unit (p.u) and the maximum and minimum line power flows are 10 kW and −10 kW, respectively. The imported power profiles of the consumers are shown in Fig.24, while the exported power profiles of the prosumers are shown in Fig.25 after implementing HEMS.

It is noted from Fig. 26 that the voltage in the buses 2,4,5 and 10 violate the maximum voltage limit of 1.05 p.u. while the network constraints were not considered. According to the network constrains in equations 38-40 that applied on the network, the voltages stay inside the limits of 0.95 p.u. to 1.05 p.u. by decreasing the amount of power injection energy by associated prosumers in different buses as shown in Fig.26. It is observed from Fig. 27 that the line power flow constraints are also satisfied in the proposed P2P energy trading approach, which may protect the power line from being over-congested in a given system. It should be noted that the violation of these constraints may adversely affect the reliability and stability of a distribution system. In that context, the proposed trading approach will enhance the power system performance in P2P energy sharing.
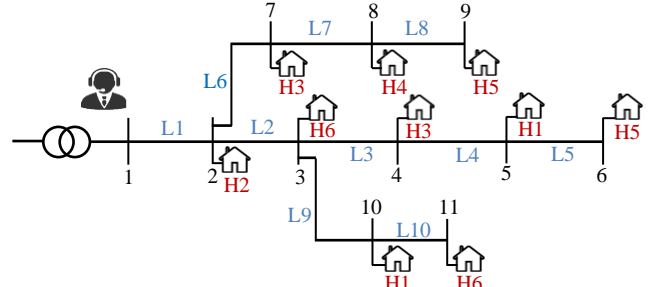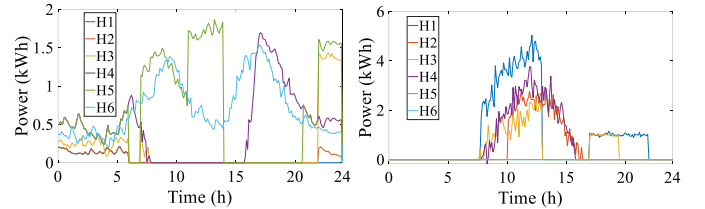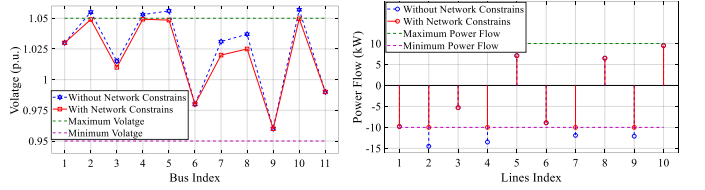
Fig. 24 Consumers' energy deficiency throughout a day.

Fig. 25 Prosumers' energy surplus throughout a day.
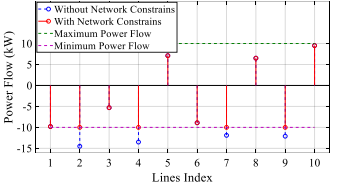
Fig. 26 Bus voltages with and without considering network constraints.

Fig. 27 Power flow in different lines with and without considering network constraints.

the Monte-Carlo simulation. The P2P energy sharing mechanism is designed based on the relationships between energy demand and supply, and Feed-in Tariff (FiT) and Real-Time Price (RTP). Furthermore, HEMS is also designed to manage the energy produced and consumed within a household. The proposed model is simulated and evaluated on a local community of 100 households subject to constraints associated with household load profile, PV, EVs, BESs and market signals including FiT and retail prices. The simulation results show that the proposed HEMS can effectively manage the energy flow within each type of household and simultaneously enable EVs to participate in P2P market. The proposed HEMS can also increase the self-consumption rate within the community which depends mainly on the batteries capacity and their SoCs. The results show that the effective performance of the proposed P2P pricing mechanism in achieving cost saving/income for consumers/prosumers with considering that not a single household would be worse off. This leads to motivates peers to participate in P2P energy trading. To validate the performance of the proposed pricing mechanism, it is evaluated by comparing to three popular P2P sharing mechanisms; the supply and demand ratio (SDR), mid-market rate (MMR) and bill sharing (BS). The simulation results verify the effectiveness the proposed mechanism in terms the economic revenue and ensure the fairness among all peers considering the physical network constrains.

V. CONCLUSION

This paper proposed a P2P energy sharing model for residential microgrids with stochastic models of different types of households equipped with PV distributed generation, EVs, and BESs to address the uncertainties using 1000 scenarios of

VI. References

[1] Zhang, C., Wu, J., Long, C., & Cheng, M. (2017). Review of existing peer-to-peer energy trading projects. Energy Procedia, 105, 2563-2568.

[2] McKenna, E., Pless, J., & Darby, S. J. (2018). Solar photovoltaic self-consumption in the UK residential sector: New estimates from a smart grid demonstration project. Energy Policy, 118, 482-491.

[3] Zhang, C., Wu, J., Long, C., & Cheng, M. (2017). Review of existing peer-to-peer energy trading projects. Energy Procedia, 105, 2563-2568.

[4] Doan, H. T., Cho, J., & Kim, D. (2021). Peer-to-Peer Energy Trading in Smart Grid Through Blockchain: A Double Auction-Based Game Theoretic Approach. IEEE Access, 9, 49206-49218.

[5] Thakur, S., Hayes, B. P., & Breslin, J. G. (2018, September). Distributed double auction for peer to peer energy trade using blockchains. In 2018 5th International Symposium on Environment-Friendly Energies and Applications (EFEA) (pp. 1-8). IEEE.

[6] Zhang, C., Yang, T., & Wang, Y. (2021). Peer-to-Peer energy trading in a microgrid based on iterative double auction and blockchain. Sustainable Energy, Grids and Networks, 27, 100524.

[7] Chen, K., Lin, J., & Song, Y. (2019). Trading strategy optimization for a prosumer in continuous double auction-based peer-to-peer market: A prediction-integration model. Applied energy, 242, 1121-1133.

[8] Angaphiwatchawal, P., Phisuthsaingam, P., & Chaitusaney, S. (2020, June). A k-Factor Continuous Double Auction-Based Pricing Mechanism for the P2P Energy Trading in a LV Distribution System. In 2020 17th International Conference on Electrical Engineering/Electronics, Computer, Telecommunications and Information Technology (ECTI-CON) (pp. 37-40). IEEE.

[9] Liu, N., Yu, X., Wang, C., Li, C., Ma, L., & Lei, J. (2017). Energy-sharing model with price-based demand response for microgrids of peer-to-peer prosumers. IEEE Transactions on Power Systems, 32(5), 3569-3583.

[10] Long, C., Wu, J., Zhou, Y., & Jenkins, N. (2018). Peer-to-peer energy sharing through a two-stage aggregated battery control in a community Microgrid. Applied energy, 226, 261-276.

[11] Long, C., Wu, J., Zhang, C., Thomas, L., Cheng, M., & Jenkins, N. (2017, July). Peer-to-peer energy trading in a community microgrid. In 2017 IEEE power & energy society general meeting (pp. 1-5). IEEE.

[12] Tushar, W., Yuen, C., Smith, D. B., & Poor, H. V. (2016). Price discrimination for energy trading in smart grid: A game theoretic approach. IEEE Transactions on Smart Grid, 8(4), 1790-1801.

[13] Tushar, W., Saha, T. K., Yuen, C., Smith, D., & Poor, H. V. (2020). Peer-to-peer trading in electricity networks: An overview. IEEE Transactions on Smart Grid, 11(4), 3185-3200.

[14] Kotani, K., Tanaka, K., & Managi, S. (2019). Which performs better under trader settings, double auction or uniform price auction?. Experimental Economics, 22(1), 247-267.

[15] Xu, S., Zhao, Y., Li, Y., & Zhou, Y. (2021). An iterative uniform-price auction mechanism for peer-to-peer energy trading in a community microgrid. Applied Energy, 298, 117088.

[16] Zhou, Y., Wu, J., & Long, C. (2018). Evaluation of peer-to-peer energy sharing mechanisms based on a multiagent simulation framework. Applied energy, 222, 993-1022.

[17] Zhang, B., Du, Y., Lim, E. G., Jiang, L., & Yan, K. (2019, November). Design and simulation of Peer-to-Peer energy trading framework with dynamic electricity price. In 2019 29th Australasian Universities Power Engineering Conference (AUPEC) (pp. 1-6). IEEE.

[18] Aznavi, S., Fajri, P., Shadmand, M. B., & Khoshkbar-Sadigh, A. (2020). Peer-to-peer operation strategy of pv equipped office buildings and charging stations considering electric vehicle energy pricing. IEEE Transactions on Industry Applications, 56(5), 5848-5857.

[19] Alfaverh, F., Denai, M., & Sun, Y. (2021). Electrical vehicle grid integration for demand response in distribution networks using reinforcement learning. IET Electrical Systems in Transportation.

[20] Li, N. (2015, December). A market mechanism for electric distribution networks. In 2015 54th IEEE Conference on Decision and Control (CDC) (pp. 2276-2282). IEEE.

[21] Ovoenergy, [Online] (2021). https://www.ovoenergy.com/guides/energy-guides/how-much-electricity-does-a-home-use Accessed December 2, 2021.

[22] "Tenure by household size by number of bedrooms," 2011. [Online]. Available:https://www.nomisweb.co.uk/census/2011/DC4405EW/view/2013265927?rows=c_sizhuk11&cols=c_bedrooms.

[23] Meng, J., Mu, Y., Jia, H., Wu, J., Yu, X., & Qu, B. (2016). Dynamic frequency response from electric vehicles considering travelling behavior in the Great Britain power system. Applied energy, 162, 966-979.

[24] "GOV.UK," Department for Transport, 30 July 2013. [Online]. Available: https://www.gov.uk/government/statistical-data-sets/nts01-average-number-of-trips-made-and-distance-travelled. [Accessed 16 August 2022].

[25] "Power Data Access Viewer," [Online]. Available: https://power.larc.nasa.gov/data-access-viewer/. [Accessed 19 August 2022].

[26] Zhou, W., Wang, Y., Peng, F., Liu, Y., Sun, H., & Cong, Y. (2022). Distribution network congestion management considering time sequence of peer-to-peer energy trading. International Journal of Electrical Power & Energy Systems, 136, 107646.

Fayiz Alfaverh received the B.Sc. degree in Electrical Power Engineering from Yarmouk University, Irbid, Jordan, , the M.Sc. degree in Power Electronics and Control Engineering from the University of Hertfordshire, Hatfield, U.K. He is currently a Ph.D student at University of Hertfordshire, Hatfield, U.K. His interests are in demand response management and control strategies for integrated smart electricty networks, and management of smart homes and dynamic scheduling, optimisation and control of future smart grids.

Mouloud Denai graduated from the University of Science and Technology of Algiers and Ecole Nationale Polythechnique of Algiers, Algeria in Electrical Engineering and received his Ph.D. in Control Engineering from the University of Sheffield, U.K. He worked for the University of Science and Technology of Oran (Algeria) until 2004 and the University of Sheffield (U.K.) from 2004 to 2010. From 2010 to 2014, he worked for the University of Teesside (U.K.). He is currently with the University of Hertfordshire (U.K.) since 2014. Dr Denai research interests in energy include intelligent control design and computational intelligence applications to efficiency optimization in renewable energy systems with particular focus in the management of smart homes and dynamic scheduling, optimization and control of future smart grids, condition monitoring and asset management in electric power networks; Energy storage systems integration into the grid; Smart meter data analytics using machine learning techniques for efficient energy management; electric vehicles integration into the distribution grid and V2G/G2V management.

Yichuang Sun (M'90-SM'99) received the B.Sc. and M.Sc. degrees from Dalian Maritime University, Dalian, China, in 1982 and 1985, respectively, and the Ph.D. degree from the University of York, York, U.K., in 1996, all in communications and electronics engineering. Dr. Sun is currently Professor of Communications and Electronics, Head of Communications and Intelligent Systems Research Group, and Head of Electronic, Communication and Electrical Engineering Division in the School of Engineering and Computer Science of the University of Hertfordshire, UK. He has published over 330 papers and contributed 10 chapters in edited books. He has also published four text and research books: Continuous-Time Active Filter Design (CRC Press, USA, 1999), Design of High Frequency Integrated Analogue Filters (IEE Press, UK, 2002), Wireless Communication Circuits and Systems (IET Press, 2004), and Test and Diagnosis of Analogue, Mixed-signal and RF Integrated Circuits - the Systems on Chip Approach (IET Press, 2008). His research interests are in the areas of wireless and mobile communications, RF and analogue circuits, microelectronic devices and systems, and machine learning and deep learning.

Appendixes

Appendix A

According to the basic principle of economics, prices decrease with higher supply/lower demand and increase with the higher demand/ lower supply. In the P2P energy market, when there is no energy surplus exported from a prosumer ($E_S(t) = 0$) to the P2P market, the P2P buying price is set to the grid price (RTP). In contrast, when there is no energy deficiency requests ($E_D(t) = 0$) from the P2P market, the P2P selling price is set to FiT. When the ESC receives both energy surplus and deficiency requests ($-1 < \alpha < 1$), the P2P prices trend tends to follow the function $\tanh(2\alpha)$. Thus, $\tanh(2\alpha)$

can be used to model the relationship between P2P prices and α/β:

$$r_b = f(\alpha,\beta) = \begin{cases} (1-\beta)\tanh(2\alpha) & ,\alpha \geq 0 \\ \beta \tanh(2\alpha) & ,\alpha < 0 \\ r_g & ,E_S = 0 \end{cases} \quad (31)$$

$$r_s = f(\alpha,\beta) = \begin{cases} \beta \tanh(2\alpha) \\ (1-\beta)\tanh(2\alpha) & ,\alpha < 0 \\ r_{ex} & ,E_D = 0 \end{cases} \quad (32)$$

Substituting $\tanh(x) = \dfrac{e^x - e^{-x}}{e^x + e^{-x}}$, in (31) and (32):

$$r_b = f(\alpha,\beta) = \begin{cases} (1-\beta)\dfrac{e^{2\alpha} - e^{-2\alpha}}{e^{2\alpha} + e^{-2\alpha}} & ,\alpha \geq 0 \\ \beta \dfrac{e^{2\alpha} - e^{-2\alpha}}{e^{2\alpha} + e^{-2\alpha}} & ,\alpha < 0 \\ r_g & ,E_S = 0 \end{cases} \quad (33)$$

$$r_s = f(\alpha,\beta) = \begin{cases} \beta \dfrac{e^{2\alpha} - e^{-2\alpha}}{e^{2\alpha} + e^{-2\alpha}} & ,\alpha \geq 0 \\ (1-\beta)\dfrac{e^{2\alpha} - e^{-2\alpha}}{e^{2\alpha} + e^{-2\alpha}} & ,\alpha < 0 \\ r_{ex} & ,E_D = 0 \end{cases} \quad (34)$$

Where α is in the range [-1, 1] as shown in Equation (26), and to convert this range to [0,1], the formula ($X_{new} = \dfrac{X_{old} - min}{max - min}$) is used:

$$r_b = f(\alpha,\beta) = \begin{cases} \dfrac{(2-\beta)e^{2\alpha} + \beta e^{-2\alpha}}{2(e^{2\alpha} + e^{-2\alpha})} & ,\alpha \geq 0 \\ \dfrac{\beta e^{2\alpha} + (1-\beta)e^{-2\alpha}}{2(e^{2\alpha} + e^{-2\alpha})} & ,\alpha < 0 \\ r_g & ,E_S = 0 \end{cases} \quad (35)$$

$$r_s = f(\alpha,\beta) = \begin{cases} \dfrac{(2-\beta)e^{2\alpha} + \beta e^{-2\alpha}}{2(e^{2\alpha} + e^{-2\alpha})} & ,\alpha \geq 0 \\ \dfrac{\beta e^{2\alpha} + (1-\beta)e^{-2\alpha}}{2(e^{2\alpha} + e^{-2\alpha})} & ,\alpha < 0 \\ r_{ex} & ,E_D = 0 \end{cases} \quad (36)$$

Finally, to map the P2P prices into $[r_{ex}, r_g]$, the formula $(X \times (max - min) + min)$ is used. The function of P2P prices can be formulated as:

$$r_b$$
$$= \begin{cases} \left(\dfrac{r_g - r_{ex}}{2}\right)\dfrac{(2-\beta)e^{2\alpha} + \beta e^{-2\alpha}}{e^{2\alpha} + e^{-2\alpha}} + r_{ex} & ,\alpha \geq 0 \\ \left(\dfrac{r_g - r_{ex}}{2}\right)\dfrac{(1+\beta)e^{2\alpha} + (1-\beta)e^{-2\alpha}}{e^{2\alpha} + e^{-2\alpha}} + r_{ex} & ,\alpha < 0 \\ r_g & ,E_S = 0 \end{cases}$$

$$r_s$$
$$= \begin{cases} \left(\dfrac{r_g - r_{ex}}{2}\right)\dfrac{(1+\beta)e^{2\alpha} + (1-\beta)e^{-2\alpha}}{e^{2\alpha} + e^{-2\alpha}} + r_{ex} & ,\alpha \geq 0 \\ \left(\dfrac{r_g - r_{ex}}{2}\right)\dfrac{(2-\beta)e^{2\alpha} + \beta e^{-2\alpha}}{e^{2\alpha} + e^{-2\alpha}} + r_{ex} & ,\alpha < 0 \\ r_{ex} & ,E_D = 0 \end{cases}$$

Appendix B

B.1: Bill sharing mechanism (BS)

In this method, the cost of electricity for a community is shared among customers based on individual customer's total energy consumption and export. The buy and sell prices for the P2P mechanism as determined by this method are given by equations (41) and (42) respectively.

$$r_b = r_g \left(\dfrac{E_D^{BFG}}{E_D}\right) \quad (37)$$

$$r_s = r_{ex} \left(\dfrac{E_S^{STG}}{E_S}\right) \quad (38)$$

E_D^{BFG} and E_S^{STG} are respectively the total energy import and export of the community from/to the grid after P2P trading. Therefore, the electricity bill of individual households is calculated as follows:

$$C^i = (E_{D_i}^{BFG}.r_g - E_{S_i}^{STG}.r_{ex}) + (E_{D_i}^{P2P}.r_b - E_{S_i}^{P2P}.r_s) \quad (39)$$

$E_{D_i}^{BFG}$ and $E_{D_i}^{P2P}$ denote the energy purchased from the main grid and P2P market by individual users respectively. $E_{S_i}^{STG}$ and $E_{S_i}^{P2P}$ are the energy sold to the main grid and P2P market respectively.

B.2: Mid-Market Rate Mechanism (MMR)

In this pricing mechanism, the P2P prices are bounded between the RTP and FiT. Therefore, the MMR method assumes that the P2P prices are set to the average value of RTP and FiT when the total energy surplus equals the energy deficiency, thus:

$$r_b, r_s = \dfrac{r_g + r_{ex}}{2} \quad (40)$$

However, the peers will buy/sell their energy under RTP/FiT in case the total energy surplus does not meet the energy deficiency in the P2P market.

B.3: Supply-Demand Ratio (SDR)

In this mechanism, P2P prices can be adjusted with the change of Supply-Demand Ratio (SDR) based on the basic principle of economics, as the relation between price and SDR is inverse-proportional. the relationship of supply and demand in the energy sharing zone can be represented by:

$$SDR = \dfrac{E_S}{E_D} \quad (41)$$

The P2P buying and selling prices are identified by equations (46) and (47) according to SDR values:

$$r_s = \begin{cases} \dfrac{r_g.r_{ex}}{(r_g - r_{ex}).SDR + r_{ex}} & ,0 \leq SDR \leq 1 \\ r_{ex} & ,SDR > 1 \end{cases} \quad (42)$$

$$r_b = \begin{cases} r_s.SDR + r_g(1 - SDR), & 0 \leq SDR \leq 0 \\ r_{ex} & SDR > 1 \end{cases} \quad (43)$$

The relationship between the internal price and SDR is shown in Fig. B.1 which shows that r_s and r_b decline with the increase of SDR in the interval [0, 1], and they are set to r_{ex} when SDR is greater than 1.
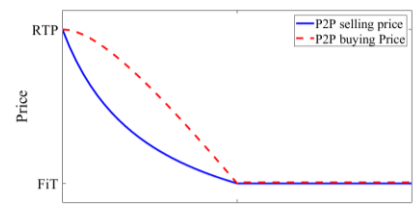

Fig. B.1 Relationship between the P2P prices and SDR.